

# Macromolecules

Volume 7, Number 5     September–October 1974

© Copyright 1974 by the American Chemical Society

## $\alpha$ - $\beta$ Transformation in Polypivalolactone

Robert E. Prud'homme and Robert H. Marchessault\*

Département de Chimie, Université de Montréal, Montréal 101, Québec, Canada.

Received February 13, 1974

**ABSTRACT:** The mechanical properties of oriented polypivalolactone (PPL) fibers are correlated with its internal structure as revealed by wide- and small-angle X-ray scattering and differential scanning calorimetry. Before cold drawing, the original melt-spun fiber was partially crystalline and its chains were oriented in a helical conformation ( $\alpha$  phase); after cold drawing, a planar zig-zag conformation is found ( $\beta$  phase) which is converted back to the  $\alpha$  phase by annealing. This  $\alpha \rightleftharpoons \beta$  transformation is similar to the one which occurs in wool. In both cases, the transformation begins in the yield region of the stress-strain curve and continues in the post-yield region.

Polyesters based on the skeletal formula  $(\text{CH}_2\text{CR}_1\text{R}_2\text{COO})_n$  exhibit a crystalline phase transformation which is analogous to the well-known  $\alpha$  to  $\beta$  transformation of keratins. The  $\alpha$  phase is characterized by a  $2_1$  helix conformation and the  $\beta$  phase by a planar zig-zag conformation. For example, it has been shown<sup>1,2</sup> that poly( $\beta$ -propiolactone) ( $\text{R}_1 = \text{R}_2 = \text{H}$ ) can be prepared predominantly in either one of these two forms depending upon the casting conditions. In addition, the  $\beta$  form is induced by cold stretching the  $\alpha$  form. The same sort of phenomenon has been reported recently for  $\alpha$ -methyl- $\alpha$ -*n*-propyl- $\beta$ -propiolactone.<sup>3-5</sup> Again, the  $\beta$  form can be induced by stretching the  $\alpha$  form.

Another member of this series, polypivalolactone ( $\text{R}_1 = \text{R}_2 = \text{CH}_3$ ) (PPL), has been reported to have two crystalline forms:<sup>6</sup>  $\alpha$  and  $\beta$ . The latter can be induced during the melt spinning of the polymer, combined with high-speed stretching. As in the previous cases, annealing of the fiber reduces the amount of  $\beta$  form. The obvious analogy of this dimorphism to the well-known helix and pleated-ribbon forms of keratins (and wool in particular) is further demonstrated by the observed conformational isomorphism for polyesters based on the  $\beta$ -propiolactone backbone, *i.e.*, with the above-mentioned skeletal formula including a polyester with a monosubstituent in the  $\beta$  position.<sup>7</sup> It is the purpose of the present paper to study this  $\alpha \rightleftharpoons \beta$  transformation of PPL using techniques such as small- and wide-angle X-ray scattering (saxr and waxr), as well as differential scanning calorimetry (DSC). In addition, the mechanical properties of the PPL fibers are measured and these are interpreted in terms of the phase transformation of the material.

### Experimental Section

Well-oriented PPL fibers were obtained from Dr. F. L. Binsbergen of the Koninklijke/Shell-Laboratorium in Amsterdam. The fibers have been spun from a polypivalolactone batch of viscosity-average molecular weight of about 250,000 containing a small amount (about 0.2% wt) of a stabilizer. During spinning a very small decrease of molecular weight was observed. After spinning, the yarn was drawn at 1:3.2 over a hot plate at 125°. The yarn has a total denier of 112 and contains 37 filaments.<sup>8a</sup>

Waxr and saxr patterns are recorded using a Picker Microfocus generator (copper target, nickel filtered) and a Warhus-Statton<sup>8b</sup> flat-plate camera, under vacuum. For the waxr work, a 0.020-in.

collimator was used, while for the saxr work, a special collimating arm was placed in front of the camera. The limit of resolution of such a saxr apparatus is about 175 Å.

DSC measurements were made on a Perkin-Elmer, Model 1B apparatus, calibrated with a tin sample whose melting point is 505°K. Stress-strain properties of the fibers were evaluated on an Instron table model "TM" tensile tester, at a stretching rate of 40%/min, and at 25°.

### Results

The first step in the analysis of the PPL fibers was made on the original sample, without further treatment. This fiber is highly crystalline and shows a fiber waxr diagram which corresponds to the  $2_1$  helical structure ( $\alpha$  phase) described in the literature.<sup>9-11</sup> Its monoclinic unit cell has the following dimensions:  $a = 9.05$  Å,  $b = 11.58$  Å,  $c = 6.03^\circ$ , and  $\beta = 121.5^\circ$ . An example of such a diagram is given in Figure 1a. Upon annealing the scattered intensity increases markedly, indicating an increase of the crystallinity of the fiber. Other workers have reported the same phenomenon.<sup>8a,12</sup>

Annealed and unannealed fibers show two symmetric diffraction maxima in the saxr diagram as presented in Figure 1c. The long period calculated from this sort of diagram depends upon annealing time and temperature as shown in Figure 2. It must be mentioned that the fibers were annealed while being kept at a fixed length and since they tended to shrink on heating they were automatically kept taut. The observed change in long spacing with annealing temperature is similar to that reported for single crystals or for the isothermal crystallization of polymers from the melt or from solution.<sup>13</sup> The same sort of phenomenon is also found for Nylon 66<sup>14</sup> and poly(ethylene terephthalate)<sup>15</sup> fibers. It indicates the presence of folded-chain lamellae oriented perpendicular to the long axis of the fiber which increase their size during annealing. It was also observed that the intensity of the saxr diagram increases with annealing.

Stretching caused important changes in the structure of the fiber. This is shown in the fiber diagram presented in Figure 1b which is typical for a sample stretched at room temperature between 10 and 100%. Two major changes are then observed: first of all, the intensity of the original reflections, characteristic of the helical structure, is significantly reduced although these diffraction spots

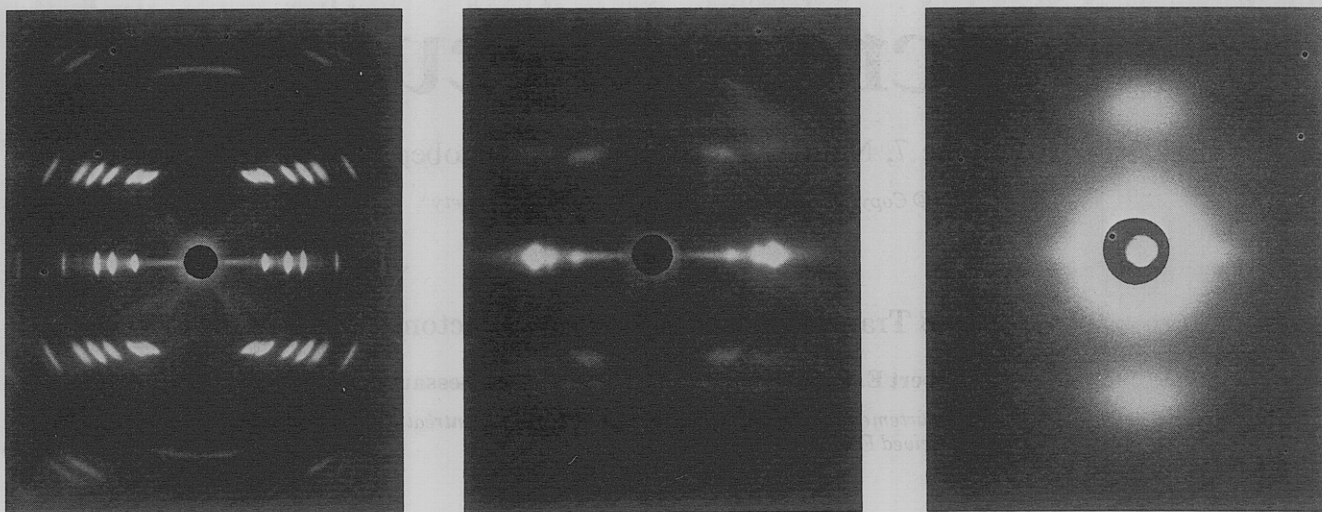


Figure 1. WAXS fiber diagram of an unstretched (a, left) and stretched (b, middle) PPL fiber; (c, right) SAXS diagram of an unstretched sample. Fiber axis is vertical in all cases.

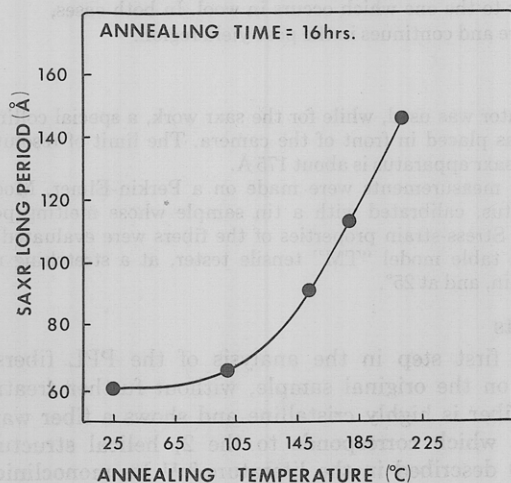


Figure 2. Variation of the SAXS long period as a function of annealing temperature.

never completely disappear. Secondly, additional reflections are present on the diagram. (i) The original 020 reflection ( $2\theta = 17.9^\circ$ ,  $d = 4.94 \text{ \AA}$ ) becomes very intense. (It is the third equatorial reflection from the center.) For the original fiber, the intensities of the first three reflections are in a ratio of 1.00:1.12:0.78. But for a stretched fiber, the intensity of the third reflection may increase by a factor of eight compared to the first (100) or second ( $1\bar{2}0$ ) reflections. (ii) A new continuous streak appears above the first layer line reflections of the original diagram. This streak corresponds to a periodicity along the fiber ( $c$ ) axis of  $4.76 \text{ \AA}$  and is equal to the repeat distance of a PPL chain in a planar-zig-zag conformation ( $\beta$  phase). Such a structure has been previously reported for a sample which has been oriented during the melt spinning operation,<sup>6</sup> but this is the first observation of the zig-zag conformation as a result of cold drawing.

In order to follow semiquantitatively the  $\alpha \rightleftharpoons \beta$  transformation in the PPL fibers, we defined in the following way the fraction of the  $\beta$  phase present

$$\text{fraction of } \beta \text{ phase} = (I_{\text{exp}} - I_{\text{theor}})/I_{\text{exp}} \quad (1)$$

where  $I_{\text{exp}}$  is the sum of the diffracted intensity for 100,  $1\bar{2}0$ , 020 reflections and is taken to be proportional to the area under the respective peaks for a microdensitometer scan along the equator;  $I_{\text{theor}}$  is the theoretical intensity and is assumed proportional to the sum of the areas under

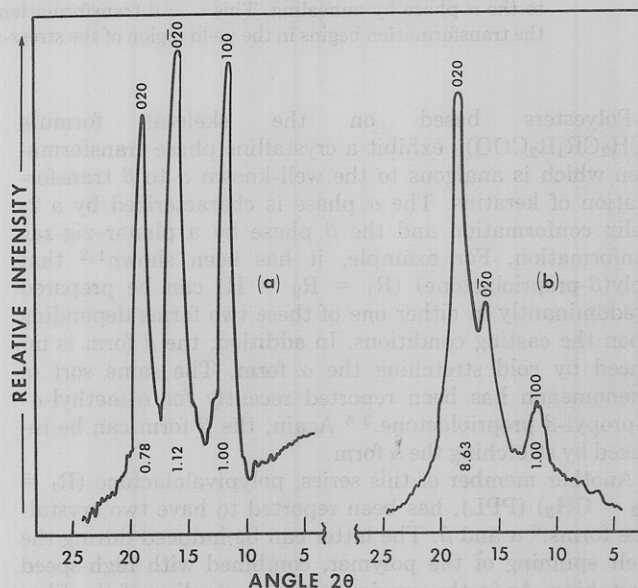


Figure 3. WAXS equatorial trace of an unstretched (a) and stretched (b) sample.

the peaks for a radial scan of the diffraction diagram given by the original fiber. From the Figure 3a and the foregoing,  $I_{\text{theor}} = 2.90$ , if we take the area of the 100 reflection peak as equal to 1.0. The measured value of  $I_{\text{exp}}$  must also be normalized for an area of 1.0 for the 100 reflection peak. For the original fiber we assume that the  $\beta$  phase is absent and  $I_{\text{exp}} = I_{\text{theor}}$  (Figure 3a). For a sample stretched 100% at room temperature  $I_{\text{exp}}$  equals 9.63 (Figure 3b), we conclude the sample contains 70% of  $\beta$  phase. It should be noted that the  $\beta$ -phase reflection at  $17.9^\circ$  is rather broad, consequently the  $1\bar{2}0$  reflection due to a  $\alpha$  phase is not well resolved appearing as a shoulder. It is clear that the fraction of  $\beta$  phase as defined by eq 1 is arbitrary. But this being understood, it is a useful definition to follow the  $\alpha \rightleftharpoons \beta$  transformation.

Because only two independent reflections appear for the zig-zag conformation it is not possible to determine its unit cell. It is clear however that this unit cell must be primitive in order to give rise to so few reflections and to a continuous streak on the first layer line. More specifically it would appear that a random translation of chains and a layered packing such as suggested for  $\alpha$ -methyl- $\alpha$ - $n$ -propyl- $\beta$ -propiolactone would best account for the data.<sup>5</sup>

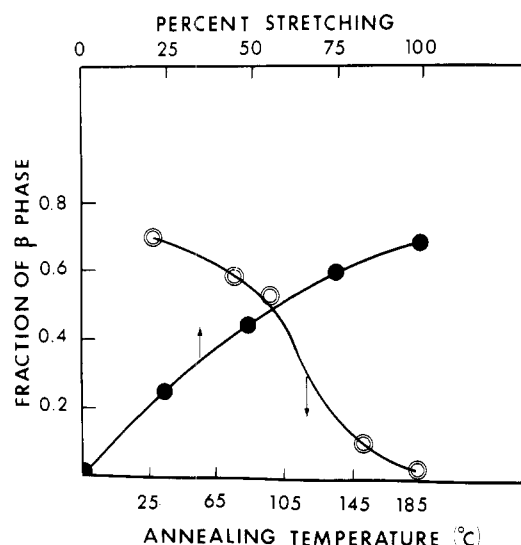


Figure 4. Measured fraction of the  $\beta$  phase as a function of (a) per cent stretching and (b) annealing temperature.

Changes in the phase structure of the PPL sample as a function of per cent stretching of the original fiber are given in Figure 4a. It is seen that the per cent of  $\beta$  phase goes from 0 to 45% in the 0-50% elongation region and from 45 to 70% in the 50-100% elongation region. The  $\alpha \rightleftharpoons \beta$  transformation is proportionately greater for small elongation ratios than for large elongations.

If we now take a sample and stretch it 100%, at room temperature, we will obtain a fiber containing 70% of the  $\beta$  phase. Upon annealing, the per cent of  $\alpha$  phase will decrease as indicated in Figure 4b. It is seen that most changes occur in the temperature range 100-150° where the  $\beta$  phase decreases from 52 to 9%. After annealing for 16 hr at 180°, the  $\beta$  phase is almost completely lost. It should be recalled that all X-ray experiments were made on samples held at constant length hence tension was maintained during annealing and after. If it is not then part of the  $\beta$  phase is lost as a function of time. For example, for the sample stretched 100% at room temperature, the initial per cent of  $\beta$  phase is 70%. After releasing the tension, at room temperature, we obtain 58 and 24% of  $\beta$  phase after 15 hr and 15 days, respectively. At higher temperature, this process will obviously be faster.

According to the conformational energy calculations of Cornibert *et al.*<sup>4,11</sup> there is no difference in enthalpy between the  $\alpha$  and  $\beta$  conformations. However, conversion between the two involves an energy barrier of about 8.0 kcal/mol of monomer. Therefore considering only the molecules themselves it is not surprising that work is required to transform from  $\alpha$  to  $\beta$ . The results of the annealing experiments suggest that free energy considerations favor the  $2_1$  conformation.

The  $\alpha \rightleftharpoons \beta$  transformation of PPL described above is shown schematically in Figure 5. The original fiber contains uniquely the  $\alpha$  phase (Figure 5a). Upon annealing, the crystallinity increases and this gives rise to a sharper fiber diagram (Figure 5c). Upon cold stretching the original fiber, the  $\beta$  phase is induced (Figure 5b). Upon annealing, the  $\beta$  phase disappears and we obtain again a pattern of similar intensity as the one obtained by annealing directly the original sample. The fiber has then lost memory of the  $\beta$  phase. This is further confirmed by the saxr measurements. From Figure 2, it is seen that the long period of the original fiber is 61 Å. After annealing at 180° the long period increases to 112 Å. For the sample stretched 100%, the saxr pattern shows only a diffuse halo, with no discrete maximum. This means that the lamellar structure has been destroyed. After annealing the

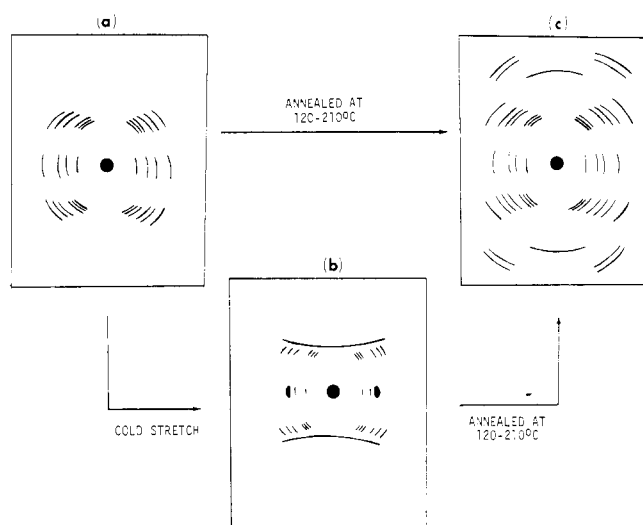


Figure 5. Schematic representation of the waxr fiber diagram obtained for: (a) the original fiber ( $\alpha$  phase); (b) the stretched fiber ( $\alpha + \beta$  phase); (c) a fiber stretched and subsequently annealed.

stretched sample at 180°, we once again obtain a long period of 112 Å.

The  $\beta$  structure can also be detected by calorimetry. As we have shown in a separate paper,<sup>16</sup> the original fiber gives a single sharp melting peak at 508°K. But the stretched sample gives two melting peaks at 508 and 512°K. On the other hand, the sample which is stretched 100% and then annealed many hours at 180° gives only the original peak at 508°K. By comparison with the X-ray data, we associated the 508°K peak with the  $\alpha$  phase, and the 512°K peak with the  $\beta$  phase. Thermodynamically one would expect the  $\alpha$  phase to have a higher melting point than the  $\beta$  phase. Reasons for this apparent contradiction are discussed in a previous paper.<sup>16</sup>

The stress-strain curves for an original monofilament (PPL-R25) and a monofilament annealed at 180° for 16 hr (PPL-R180) are presented in Figure 6. Both measurements were made at 25° and a stretching rate of 40%/min. In both cases, three distinct regions can be seen. For the 0-2.5% elongation region, a rapid increase in tension is observed. This is associated with the elastic deformation of the filament involving the orientation of the crystalline and amorphous regions of the sample. This is followed by a yield region ranging from 2.5% to about 50% elongation. This region is characterized by an almost constant value of the tension for the unannealed sample and a small increase of tension for the annealed sample. As seen in Figure 4a, this is the region where the  $\alpha \rightleftharpoons \beta$  transformation predominantly takes place. As we will discuss more extensively shortly, this transformation is responsible for the plateau of the yield region. The yield region starts sooner in the annealed sample since it is more crystalline and its elastic deformation is more limited. Because of this greater rigidity of the annealed sample, the  $\alpha \rightleftharpoons \beta$  transformation is accompanied by an additional increase in tension. This can also be related to a greater degree of chain unfolding than in the unannealed sample. These two regions are followed by a post-yield region and break. In the post-yield region, the tension increases rapidly. Since the annealed sample is more rigid and contains more perfect crystals, the slope of its post-yield region is greater. It also breaks at smaller elongations (range 50-75%) than the unannealed sample (range 50-150%). (The break point is not reproducible on single filaments.) This is associated with the plastic deformation behavior of semicrystalline materials where the stress relaxation processes require more time with increasing crystallinity. The post-yield region

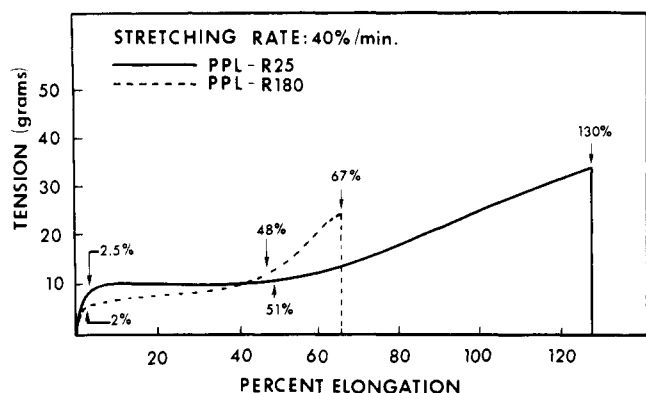


Figure 6. Stress-strain curve of a PPL single filament.

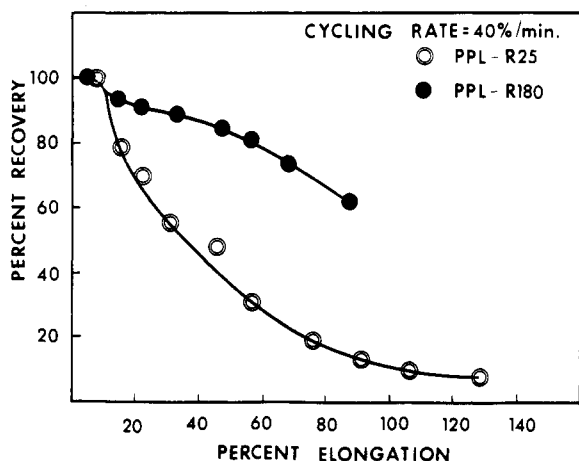


Figure 7. Strain recovery as a function of the initial elongation.

may be predominantly associated with the unfolding process. This is shown by saxr data where the long period was found to increase slightly in the yield region, but disappear in the post-yield region indicating the destruction of well defined lamellae. This will be discussed in more detail shortly. It can however be noted that such stress-strain curves have been reported by Clark<sup>17</sup> who also indicated the increase of the long period with stretching and the absence of a discrete saxr maximum for the highly stretched materials made predominantly of the  $\beta$  structure.<sup>18</sup>

Cyclic loading experiments were also performed. The yarns were strained to a tension  $T_1$ , then the strain was released to zero tension; the yarn was restrained to a tension  $T_2$  where  $T_2 > T_1$ , and the strain was again released to zero tension, and so on. In the elastic region, the strain recovery was complete; however for larger elongations, the strain recovery was only partial. From such cyclic loading experiments, we determined the strain recovery curves which are presented in Figure 7. For the unannealed yarn, the strain recovery decreases very rapidly as a function of initial elongation; for a 100% initial elongation, the annealed yarn shows a much better recovery which is still of the order of 62%. This is in agreement with the findings of Knoblock and Statton<sup>6</sup> and Clark,<sup>17,18</sup> who indicated that annealing is necessary in order to get a "high work recovery elastic fiber."

### Discussion and Conclusion

In the previous section, we have indicated conditions permitting an  $\alpha \rightleftharpoons \beta$  transformation in PPL fibers. From waxr and saxr data, it was shown that the original fiber is made of folded chain lamellae which are in an helical conformation ( $\alpha$  phase). On the other hand, the cold-drawn

	CHAIN MORPHOLOGY	CHAIN CONFORMATION
(A) INITIAL FIBER		
(B) YIELD REGION		
(C) POST-YIELD REGION		

Figure 8. Models for the chain morphology and the chain conformation of an unannealed PPL fiber as a function of elongation. The original fiber has only helical chains while in the "yield" and "post-yield" regions both helical and planar-zig-zag chain conformations are present.

fiber (100%) has extended chains which are predominantly in a planar-zig-zag conformation. The stretching operation brings about change at two different levels: morphological and conformational. The  $\alpha \rightleftharpoons \beta$  transformation predominates in the yield region of the stress-strain curve (Figure 4a) and the chain unfolding process in the post-yield region. This is indicated by the fact that only minor changes are observed in the saxr diagram in the yield region, but that the saxr peak soon disappears in the post-yield region.

These observations must be put in parallel with the stress-strain curves. We first notice that the plateau region of the yield zone is unusual for fibers.<sup>19</sup> In fact, to the authors' knowledge, this is only found for wool,<sup>19,20</sup> where an  $\alpha \rightarrow \beta$  transformation also takes place. It is believed that the yield region of wool involves an opening up of the chains from the  $\alpha$  conformation to the  $\beta$  conformation, which coexist in the system. This transformation is energetically favored. As a function of stretching, the proportion of the  $\beta$  structure increases and the stress level is fixed by the free-energy difference between the two phases. The degree of extension only determines the proportion of the structure in each of the phases. The  $\alpha \rightarrow \beta$  transformation continues further in the post-yield region where additional effects occur involving an increase of tension. This latter portion of the curve is still a matter of discussions.<sup>20-23</sup> But it is well accepted that folded chains do not exist in wool. On the other hand, the deformation of synthetic fibers such as Nylon 66<sup>14</sup> and poly(ethylene terephthalate)<sup>15</sup> involves mainly the unfolding of chains.

This is associated with a continuous increase of tension with elongation.

In view of the data presented above, we propose for the PPL fibers the deformation mechanism described schematically in Figure 8. The initial fiber is highly crystalline and made of lamellae. Its chain is completely in an helical conformation (Figure 8a). In the yield region, the elongation induces a planar-zig-zag conformation in small sections of the chains which open up exactly as in wool (Figure 8b). As elongation increases, many different sections of the same chain may open, or the opening may propagate from a given point in a single chain. The stress remains constant during this process because there exists an equilibrium between the two phases. The stress level is fixed by the free-energy difference between the phases and the mechanical extension determines the proportion of the structure in each of the phases.<sup>20-23</sup> Around 50% elongation, when about 45% of the crystalline chains have been converted into the  $\beta$  phase, the  $\alpha = \beta$  equilibrium is disrupted and unfolding of the chains becomes important (Figure 8c). This is accompanied by an increase of the stress. The passage of the yield region to the post-yield region may be due to the presence of chain entanglements and to the higher rigidity of the system under large extensions. The chains do not have enough mobility to change phase when folded. Unfolding then occurs, accompanied by an increase of stress, and possibly followed by a phase transformation of the free chain (with constant stress level). This process may be repeated many times. The break point always occurs before the complete transformation into the  $\beta$  phase is achieved. Complete chain unfolding is probably not achieved either.

Clark previously reported a row structure for PPL fibers<sup>17,18</sup> and a deformation mechanism which is quite different from the one proposed above. We believe that we are dealing with a different structure. (a) Clark studied the "high work recovery elastic (PPL) fiber," as shown in Figure 7, the annealed PPL sample, which we used, shows high recovery, but not the unannealed sample for which most of our data are obtained. The deformation mechanism proposed above holds uniquely for the latter. (b) The row model of Clark implies that the fibers do not neck upon elongation (constant diameter). This condition was met with Clark's fibers, but not in our experiments. (c) Upon heating, our PPL shrink significantly indicating extended, strained macromolecules. Upon heating, Clark's strained sample released stress indicating its energy-based recovery forces.

For the reasons mentioned above, we believe that the structure of the unannealed PPL fiber studied in this

paper is similar to that of Nylon 66<sup>14</sup> or poly(ethylene terephthalate)<sup>15</sup> fibers, except for the  $\alpha = \beta$  transformation which adds a special dimension to its deformation behavior. On the other hand, the structure of the annealed PPL fiber and consequently its deformation behavior most probably agree with the row structure model of Clark.<sup>18</sup>

The differences in structure of the unannealed and annealed PPL fibers as studied by Clark<sup>17,18</sup> and by the present authors in this paper, emphasize again the importance of heat treatment on the morphology of polymer systems. Not only is it possible to increase crystallinity and to thicken lamellae during annealing, but it also seems possible to produce quite different morphology. The transformation from the morphology here described to the "row" structure is not yet understood.

## References and Notes

- (1) K. Wasai, T. Saegusa, and J. Furukawa, *Kogyo Kagaku Zasshi*, **67**, 601 (1964).
- (2) T. Kagiya, T. Sano, and K. Fukui, *Kogyo Kagaku Zasshi*, **67**, 451 (1964).
- (3) A. E. Allegrezza, Ph. D. Thesis, University of Massachusetts (1972).
- (4) J. Cornibert, Thèse de Doctorat, Université de Montréal (1972).
- (5) J. Cornibert, R. H. Marchessault, A. E. Allegrezza, and R. W. Lenz, *Macromolecules*, **6**, 676 (1973).
- (6) F. W. Knoblock and W. O. Statton, U. S. Patent 3,299,171 (1967).
- (7) J. Cornibert and R. H. Marchessault, *J. Mol. Biol.*, **71**, 735 (1972).
- (8) (a) F. L. Binsbergen, Koninklijke/Shell-Laboratorium, Amsterdam, private communication. (b) Manufactured by W. H. Warhus, Carcroft, Del.
- (9) G. Carazzolo, *Chim. Ind.*, **46**, 525 (1964).
- (10) G. Perego, A. Melis, and M. Cesari, *Makromol. Chem.*, **1157**, 269 (1972).
- (11) J. Cornibert, N. V. Hien, F. Brisse, and R. H. Marchessault, to be published.
- (12) C. Borri, S. Brückner, V. Crescenzi, G. Bella Fortuna, A. Mariano, and P. Scarazzato, *Eur. Polym. J.*, **7**, 1515 (1971).
- (13) P. H. Geil, "Polymer Single Crystals," Wiley-Interscience, New York, N. Y., 1963.
- (14) P. F. Dismore and W. O. Statton, *J. Polym. Sci., Part C*, **13**, 133 (1966).
- (15) W. O. Statton, J. L. Koenig, and M. J. Hannon, *J. Appl. Phys.*, **41**, 4290 (1970).
- (16) R. E. Prud'homme and R. H. Marchessault, *Makromol. Chem.*, in press.
- (17) E. S. Clark, "Elastic Deformation of Crystalline Polymers: Row Structure Elasticity," presented at the Conference on "The Role of Crystallinity in Governing Polymer Properties," at the University of Utah, July 1971.
- (18) E. S. Clark in "Structure and Properties of Polymer Films," R. W. Lenz and R. S. Stein, Ed., Plenum Press, New York, N. Y., 1973, pp 267-282.
- (19) L. Rebenfeld in "Polymer Science and Materials," A. V. Tobolsky and H. F. Mark, Ed., Wiley-Interscience, New York, N. Y., 1971, pp 351-381.
- (20) B. M. Chapman and M. Feughelman, *J. Polym. Sci., Part C*, **20**, 189 (1967).
- (21) J. W. S. Hearle, *J. Polym. Sci., Part C*, **20**, 215 (1967).
- (22) A. Ciferri, *Trans. Faraday Soc.*, **59**, 562 (1963).
- (23) B. M. Chapman, *J. Text. Inst.*, **60**, 181 (1969).